Белорусский государственный университет
Минск
6.04.2010 г.

UNIVERSITÉ DU LUXEMBOURG

БИОИНФОРМАТИКА – ИНТЕЛЛЕКТУАЛЬНЫЙ АНАЛИЗ БИОСИСТЕМ

Н.Н. Яцков[1], П.В. Назаров[3], А.А. Головатый[2], Л. Валлар[3], Э. Фридерих[2], В.В. Апанасович[1]

[1] Кафедра системного анализа, БГУ, Минск, Беларусь
[2] Cytoskeleton and Cell Plasticity Laboratory, University of Luxembourg, Luxembourg
[2] Microarray Center, CRP-Sante, Luxembourg

«ИНФОРМАЦИОННЫЕ ТЕХНОЛОГИИ, ЭЛЕКТРОННЫЕ ПРИБОРЫ И СИСТЕМЫ» (ITEDS'2010)
6–7 апреля 2010 г., Минск, Беларусь

CRP SANTÉ
CENTRE DE RECHERCHE PUBLIC

Общая информация

- **Биоинформатика** – научное направление, целью которого является разработка алгоритмов для анализа и систематизации генетической информации.

- Полученные алгоритмы используются для определения структур белков и макромолекул, генетических сетей и их функций, с целью объяснения различных биологических процессов.

Генетические сети

Генетическая сеть

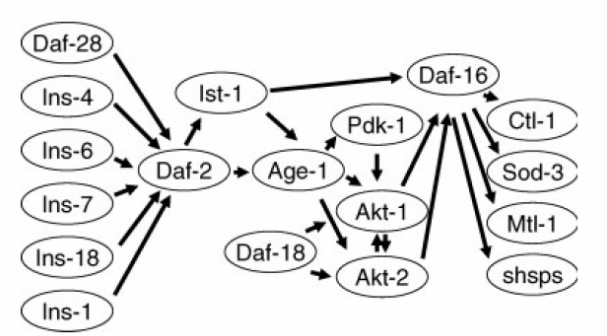

Геном

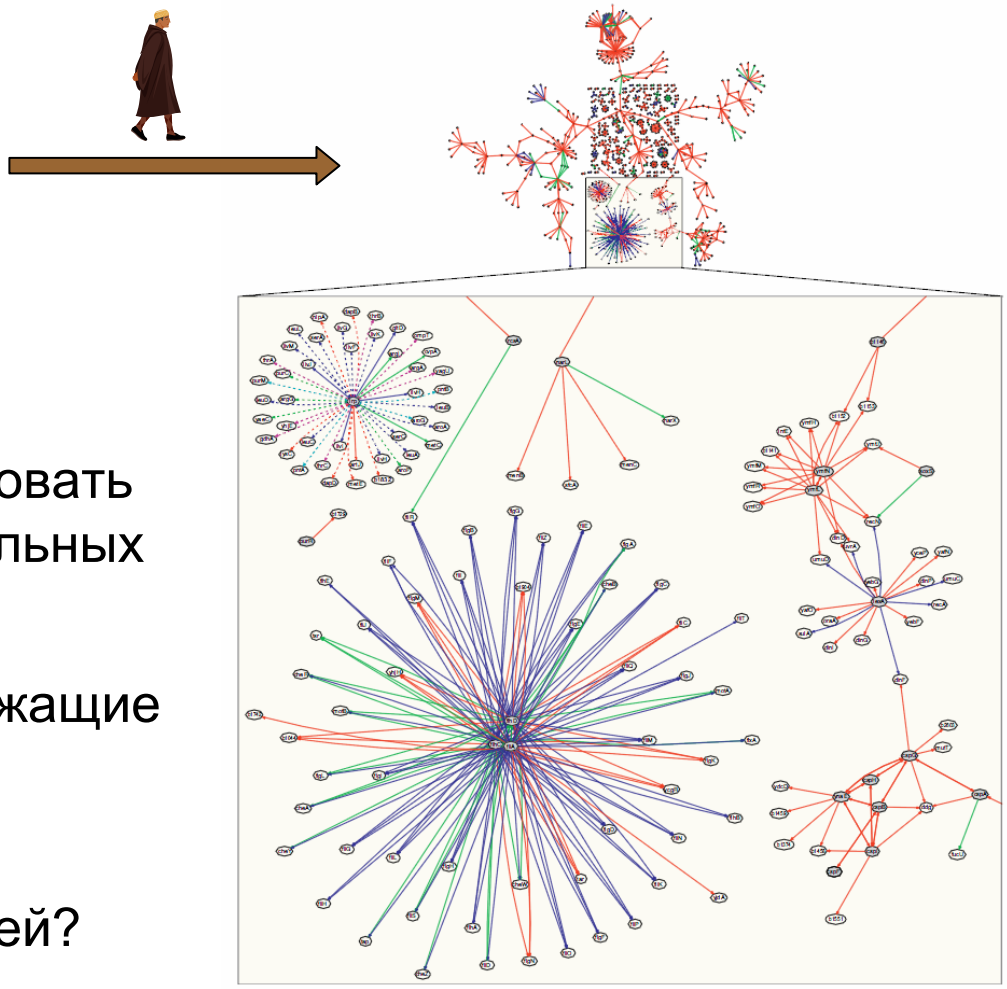

Ключевые вопросы:

- Каким образом трансформировать информацию об экспериментальных данных в сети?
- Как подтвердить гипотезы лежащие в основе сетей?
- Каким образом использовать информацию генетических сетей?

Биоинформатика

Многоуровневые мат. модели биосистем

$$A = \{k_{SNUC}, k_{DITP}, k_{ASTP}, k_{DITB}, k_{ASTB}\}$$

$z_1(t)$: $d[ATM]_t/dt = f_1(A, [ATM]_t, [ATF]_t, [FTB]_t, [FTP]_t)$
$z_2(t)$: $d[ATF]_t/dt = f_2(A, [ATM]_t, [ATF]_t, [FTB]_t, [FTP]_t)$
$z_3(t)$: $d[FTB]_t/dt = f_3(A, [ATM]_t, [ATF]_t, [FTB]_t, [FTP]_t)$
$z_4(t)$: $d[FTP]_t/dt = f_4(A, [ATM]_t, [ATF]_t, [FTB]_t, [FTP]_t)$

$$\Omega = [T_0, T]$$

Разработка биочипов

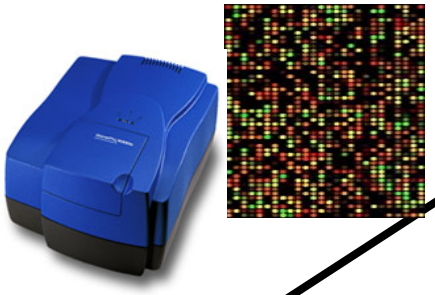

Люминесцентная микроскопия

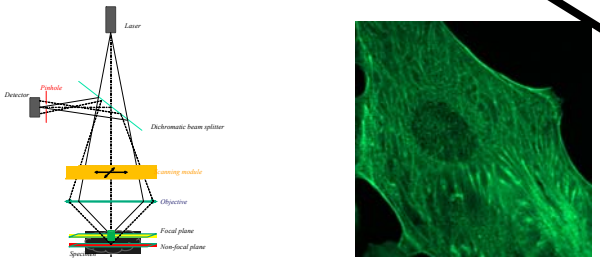

Анализ данных

Моделирование генетических сетей

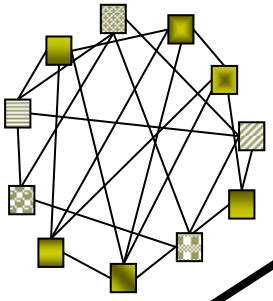

Анализ генной аннотации

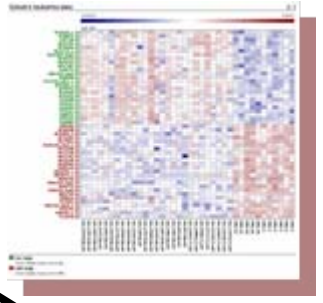

Мета-анализ данных

Базы данных

Микроматрицы ДНК

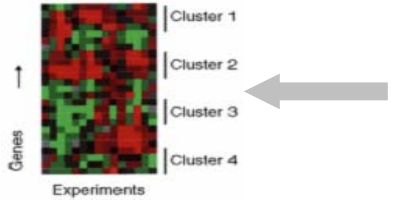

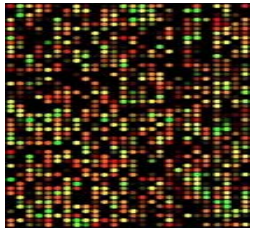

BMC Genomics 2007, 8:294

BMC Genomics

BioMed Central

Methodology article

Open Access

Design and evaluation of Actichip, a thematic microarray for the study of the actin cytoskeleton

Jean Muller[1,2,4], André Mehlen[1], Guillaume Vetter[1,3], Mikalai Yatskou[1], Arnaud Muller[1], Frédéric Chalmel[2,5], Olivier Poch[2], Evelyne Friederich[1,3] and Laurent Vallar*[1]

Address: [1]Laboratoire de Biologie Moléculaire, d'Analyse Génique et de Modélisation, Centre de Recherche Public-Santé, 84 rue Val Fleuri, L-1526 Luxembourg, Luxembourg, [2]Laboratoire de Bioinformatique et Génomique Intégratives, Institut de Génétique et de Biologie Moléculaire et Cellulaire, Inserm, U596; CNRS, UMR7104, F-67400 Illkirch, Université Louis Pasteur, F-67000 Strasbourg, France, [3]Cytoskeleton and cell plasticity laboratory, Life Sciences RU, University of Luxembourg, 162a Avenue de la faïencerie, L-1511 Luxembourg, Luxembourg, [4]Computational Biology Unit, European Molecular Biology Laboratory, Meyerhofstrasse 1, D-69117 Heidelberg, Germany and [5]GERHM-Inserm U625, Université Rennes I, Campus de Beaulieu, Bt 13, Avenue du Général Leclerc, F-35042 Rennes cedex, France

Email: Jean Muller - jean.muller@embl.de; André Mehlen - andre.mehlen@crp-sante.lu; Guillaume Vetter - guillaume.vetter@uni.lu; Mikalai Yatskou - mikalai.yatskou@crp-sante.lu; Arnaud Muller - arnaud.muller@crp-sante.lu; Frédéric Chalmel - frederic.chalmel@univ-rennes1.fr; Olivier Poch - olivier.poch@igbmc.u-strasbg.fr; Evelyne Friederich - evelyne.friederich@uni.lu; Laurent Vallar * - laurent.vallar@crp-sante.lu

* Corresponding author

Published: 29 August 2007

BMC Genomics 2007, 8:294 doi:10.1186/1471-2164-8-294

Received: 29 January 2007

Accepted: 29 August 2007

This article is available from: http://www.biomedcentral.com/1471-2164/8/294

Abstract

Background: The actin cytoskeleton plays a crucial role in supporting and regulating numerous cellular processes. Mutations or alterations in the expression levels affecting the actin cytoskeleton system or related regulatory mechanisms are often associated with complex diseases such as cancer. Understanding how qualitative or quantitative changes in expression of the set of actin cytoskeleton genes are integrated to control actin dynamics and organisation is currently a challenge and should provide insights in identifying potential targets for drug discovery. Here we report the development of a dedicated microarray, the Actichip, containing 60-mer oligonucleotide probes for 327 genes selected for transcriptome analysis of the human actin cytoskeleton.

Results: Genomic data and sequence analysis features were retrieved from GenBank and stored in an integrative database called Actinome. From these data, probes were designed using a home-made program (CADO4MI) allowing sequence refinement and improved probe specificity by combining the complementary information recovered from the UniGene and RefSeq databases. Actichip performance was analysed by hybridisation with RNAs extracted from epithelial MCF-7 cells and human skeletal muscle. Using thoroughly standardised procedures, we obtained microarray images with excellent quality resulting in high data reproducibility. Actichip displayed a large dynamic range extending over three logs with a limit of sensitivity between one and ten copies of transcript per cell. The array allowed accurate detection of small changes in gene expression and reliable classification of samples based on the expression profiles of tissue-specific genes. When compared to two other oligonucleotide microarray platforms, Actichip showed similar sensitivity and concordant expression ratios. Moreover, Actichip was able to discriminate the highly similar actin isoforms whereas the two other platforms did not.

Conclusion: Our data demonstrate that Actichip is a powerful alternative to commercial high density microarrays for cytoskeleton gene profiling in normal or pathological samples. Actichip is available upon request.

Анализ биочипов

Data (*.tif)

1. Quantification

2. Filtering (bad spots)

3. Normalization

4. Pre-treatment

5. Control of reproducibility

6. Differential analysis

7. Filtering (invariant genes)

8. Cluster analysis

Clusters of genes

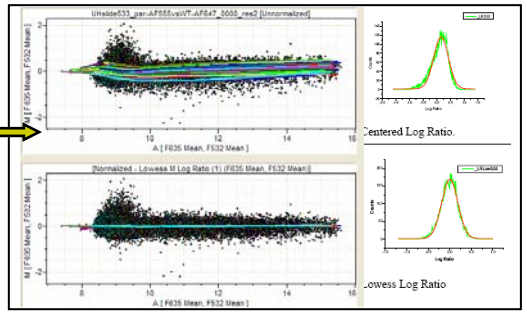

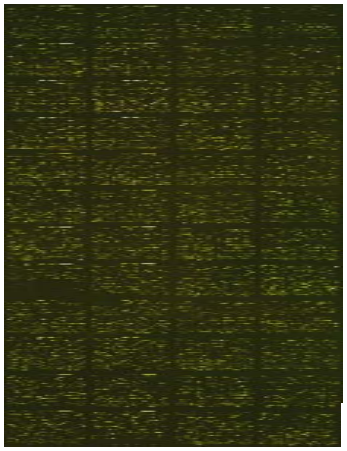

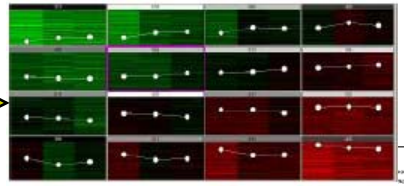

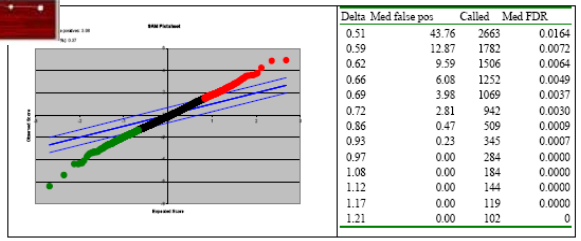

Delta Med false pos	Called	Med FDR
0.51	43.76	2663	0.0164
0.59	12.87	1782	0.0072
0.62	9.59	1506	0.0064
0.66	6.08	1252	0.0049
0.69	3.98	1069	0.0037
0.72	2.81	942	0.0030
0.86	0.47	509	0.0009
0.93	0.23	345	0.0007
0.97	0.00	284	0.0000
1.08	0.00	184	0.0000
1.12	0.00	144	0.0000
1.17	0.00	119	0.0000
1.21	0.00	102	0

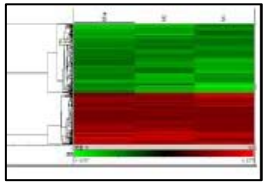

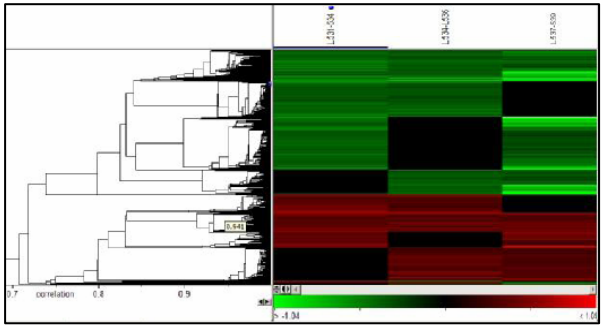

BMC Res Notes 2008, 1:80

BMC Research Notes

BioMed Central

Short Report

Open Access

Advanced spot quality analysis in two-colour microarray experiments

Mikalai Yatskou[1,2], Eugene Novikov[3,4,5], Guillaume Vetter[1,2], Arnaud Muller[1], Emmanuel Barillot[3,4,5], Laurent Vallar[1] and Evelyne Friederich*[1,2]

Address: [1]Microarray Center/LBMACM, CRP-Santé, 84 Rue Val Fleuri, L-1526, Luxembourg, [2]Cytoskeleton and Cell Plasticity Laboratory, Life Sciences Research Unit, University of Luxembourg, 162A Avenue de la Faïencerie, L-1511, Luxembourg, [3]Institut Curie, Service Bioinformatique, Institute Curie, 26 Rue d'Ulm, Paris, F-75248, France, [4]INSERM, U900, Paris, F-75248, France and [5]École des Mines de Paris, Fontainebleau, F-77300, France

Email: Mikalai Yatskou - mikalai.yatskou@uni.lu; Eugene Novikov - eugene.novikov@curie.fr; Guillaume Vetter - guillaume.vetter@uni.lu; Arnaud Muller - arnaud.muller@crp-sante.lu; Emmanuel Barillot - emmanuel.barillot@curie.fr; Laurent Vallar - laurent.vallar@crp-sante.lu; Evelyne Friederich* - evelyne.friederich@uni.lu

* Corresponding author

Published: 17 September 2008

BMC Research Notes 2008, 1:80 doi:10.1186/1756-0500-1-80

Received: 20 June 2008

Accepted: 17 September 2008

This article is available from: http://www.biomedcentral.com/1756-0500/1/80

Abstract

Background: Image analysis of microarrays and, in particular, spot quantification and spot quality control, is one of the most important steps in statistical analysis of microarray data. Recent methods of spot quality control are still in early age of development, often leading to underestimation of true positive microarray features and, consequently, to loss of important biological information. Therefore, improving and standardizing the statistical approaches of spot quality control are essential to facilitate the overall analysis of microarray data and subsequent extraction of biological information.

Findings: We evaluated the performance of two image analysis packages MAIA and GenePix (GP) using two complementary experimental approaches with a focus on the statistical analysis of spot quality factors. First, we developed control microarrays with a priori known fluorescence ratios to verify the accuracy and precision of the ratio estimation of signal intensities. Next, we developed advanced semi-automatic protocols of spot quality evaluation in MAIA and GP and compared their performance with available facilities of spot quantitative filtering in GP. We evaluated these algorithms for standardised spot quality analysis in a whole-genome microarray experiment assessing well-characterised transcriptional modifications induced by the transcription regulator SNAI1. Using a set of RT-PCR or qRT-PCR validated microarray data, we found that the semi-automatic protocol of spot quality control we developed with MAIA allowed recovering approximately 13% more spots and 38% more differentially expressed genes (at FDR = 5%) than GP with default spot filtering conditions.

Conclusion: Careful control of spot quality characteristics with advanced spot quality evaluation can significantly increase the amount of confident and accurate data resulting in more meaningful biological conclusions.

A time-resolved genome-scale study using human breast carcinoma cells

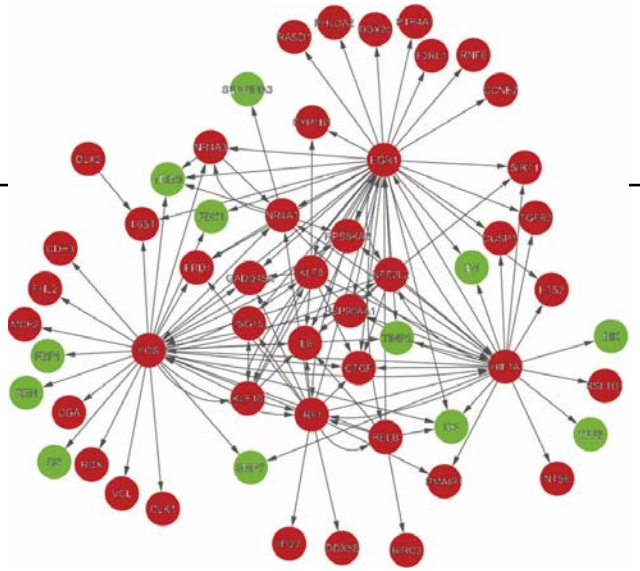

Biochem Biophys Res Comm 2009, vol 385, p.385

lated at intermediate and late stages were annotated to regulation of the cell cycle, cell growth and differentiation terms. The most represented terms for late upregulated genes were cell adhesion, and regulation of transcription.

These results suggested that SNAI1 orchestrates the balance between genes which positively or negatively regulate processes such as cell adhesion and motility, cell cycle and cell growth.

Table 1
Gene Ontology analysis of stable gene profiles. Each stable gene profile was annotated with Gene Ontology (GO), using KOBAS ANDRA module of MeMA environment, with a p-value threshold of 0.01. "GOacc" and "GOname" columns indicate GO accession number and name, respectively. The "p-value" column, obtained using a Fisher's exact test, represents the over-representation of each GO term, showing that regulated genes are associated with biological processes involved in EMT.

GOacc	p-value	GOname
DOWN early profile		
GO:0007010	4.74E−04	Cytoskeleton organization and biogenesis
GO:0006917	5.40E−03	Induction of apoptosis
GO:0006928	8.45E−03	Cell motility
GO:0007166	1.71E−02	Cell surface receptor linked signal transduction
GO:0007155	3.43E−02	Cell adhesion
GO:0006954	3.50E−02	Inflammatory response
DOWN intermediate profile		
GO:0000086	2.56E−04	G2/M transition of mitotic cell cycle
GO:0042127	7.95E−04	Regulation of cell proliferation
GO:0030216	1.50E−03	Keratinocyte differentiation
GO:0007049	5.38E−03	Cell cycle
GO:0001558	2.13E−02	Regulation of cell growth
GO:0009653	2.54E−02	Morphogenesis
GO:0007165	2.55E−02	Signal transduction
DOWN late profile		
GO:0007049	1.08E−08	Cell cycle
GO:0008284	1.85E−04	Positive regulation of cell proliferation
GO:0007067	2.45E−04	Mitosis
GO:0051301	6.48E−04	Cell division
GO:0008283	2.26E−03	Cell proliferation
UP early profile		
GO:0007166	3.55E−04	Cell surface receptor linked signal transduction
GO:0008284	2.22E−03	Positive regulation of cell proliferation
GO:0007049	4.90E−03	Cell cycle
GO:0030154	3.83E−02	Cell differentiation
UP late profile		
GO:0045449	2.21E−05	Regulation of transcription
GO:0007275	4.45E−03	Development
GO:0007155	6.23E−03	Cell adhesion

associated genes, 40 genes were identified as differentially expressed and 37 genes were associated with EMT stages (using a threshold of 1; red: upregulated genes; green: downregulated genes). A gradient from green to red indicates gene expression levels expressed as Log 2 ratios. The "Stage" column indicates gene associations (green: downregulated, red: upregulated, yellow: invariant) with early, intermediate or late EMT stages (E, I, and L).

Symbol	Early		Intermediate		Late	Stage		
	T4H	T8H	T12H	T24H	T98H	E	I	L
EGR1	3.322	2.524	1.332	1.135	-1.521			
HIF1A	2.882	2.524	2.118	1.936	1.57			
THBD	2.388	1.529	1.31	2.1	4.414			
SNAI2	2.304	1.421	1.6	1.262	1.913			
ROCK2	2.263	3.412	3.126	2.807	4.454			
RICTOR	1.89	2.17	1.118	1.218	0.029			
SNAI1	1.549	1.366	1.712	0.947	0			
MITF	1.448	1.87	1.748	2.314	2.96			
CAV1	1.304	1.707	1.816	1.559	0.468			
CAV2	1.195	1.39	2.135	2.45	1.514			
CD44	1.109	1.687	2.101	2.455	2.985			
ITGA5	1.408	0.255	1.719	1.514	0.822			
MSX1	1.234	0.846	1.813	2.385	3.394			
FOXA1	0.798	0.805	-0.585	-0.127	-2.987			
PTK2	0.806	0.53	0.443	1.003	0.897			
RAPTOR	0.472	0.234	0.158	0.832	0.642			
CDH1	0.416	0.109	-0.934	-0.862	-1.425			
GSN	0.244	0.62	-0.769	-1.011	-0.837			
CLDN7	0.227	-0.239	-1.857	-1.431	-1.809			
KRT18	0.227	-1.18	-2.725	-2.864	-2.782			
CGN	0.175	-0.414	-1.817	-1.789	-1.424			
FGFR2	0.124	0.93	0.971	1.102	2.096			
KRT3	0.099	0.116	-0.735	-0.776	-0.834			
ABLIM1	0.054	-0.317	-1.281	-1.02	-1.263			
CLDN4	-0.027	-0.859	-2.519	-2.907	-2.137			
ARNT	-0.158	-0.265	-0.407	0.308	-0.297			
KRT7	-0.22	0.059	-0.523	-0.433	-2.092			
TIMP1	-0.392	-0.452	0.039	0.347	1.231			
PKP2	-0.564	0.254	-0.808	-1.283	-1.627			
FN1	-0.802	-0.058	-0.407	-0.073	2.46			
TP53	-0.824	-0.84	-0.974	-0.996	-0.587			
SLC27A2	-0.921	-0.241	-1.897	-1.92	-0.381			
PUMA	-1.022	-0.831	-1.171	-1.371	-0.578			
KRT13	-1.033	-0.488	-0.787	-0.639	-0.903			
KRT12	-1.032	-1.213	-3.088	-3.301	-2.329			
TJP3	-1.504	-1.512	-2.427	-2.869	-2.153			
ID3	-1.848	-2.841	-0.377	-0.249	3.451			
BID	-1.926	-1.938	-3.133	-3.316	-3.375			
ID1	-2.167	-2.305	0.231	0.673	3.206			
ITGB6	-2.407	-4.449	-5.174	-5.291	-4.507			
CLDN3	-2.49	-1.901	-4.403	-5.399	-4.625			
ID2	-3.023	-2.526	-2.123	-1.992	1.803			
TFF3	-3.069	-2.781	-3.55	-3.091	-3.141			
BMP7	-4.633	-3.77	-3.599	-3.026	-2.194			

Biochemical and Biophysical Research Communications 385 (2009) 485–491

Contents lists available at ScienceDirect

Biochemical and Biophysical Research Communications

journal homepage: www.elsevier.com/locate/ybbrc

Time-resolved analysis of transcriptional events during SNAI1-trigger epithelial to mesenchymal transition

G. Vetter[a,1], A. Le Béchec[b], J. Muller[b,c,2], A. Muller[a], M. Moes[a], M. Yatskou[a], Z. Al Tanoury[a], O. Poch[c], L. Vallar[a], E. Friederich[a]

[a] Cytoskeleton and Cell Plasticity Lab, Life Sciences Research Unit-FSCT, University of Luxembourg, L-1511 Luxembourg, Luxembourg
[b] Centre de Recherche Public Santé, 84, Val Fleuri, L-1526 Luxembourg, Luxembourg
[c] IGBMC, Laboratoire de Bioinformatique et de Génomique Intégratives Illkirch F-67404, France

ARTICLE INFO

Article history:
Received 6 May 2009
Available online 12 May 2009

Keywords:
Epithelium to mesenchyme transition
SNAI1
Microarray
Functional genomics

ABSTRACT

The transcription regulator SNAI1 triggers a transcriptional program leading to epithelial to mesenchymal transition (EMT), providing epithelial cells with mesenchymal features and invasive properties during embryonic development and tumor progression.

To identify early transcriptional changes occurring during SNAI1-induced EMT, we performed a time-resolved genome-scale study using human breast carcinoma cells conditionally expressing SNAI1. The approach we developed for microarray data analysis, allowed identifying three distinct EMT stages and the temporal classification of genes. Importantly, we identified unexpected, biphasic expression profiles of EMT-associated genes, supporting their pivotal role during this process. Finally, we established early EMT gene networks by identifying transcription factors and their potential targets which may orchestrate early events of EMT. Collectively, our work provides a framework for the identification and future systematic analysis of novel genes which contribute to SNAI1-triggered EMT.

Полимеризация актина

Функции актина

- Форма клетки, морфогенезиз
- Миграция, сцепление
- Передача биологических сигналов
- Заболевания (рак, воспаление)

Актин способен

- Формировать динамические структуры
- Самоорганизовываться в филаменты (белковые нити)
- Определять инвазию нормальных и злокачественных клеток

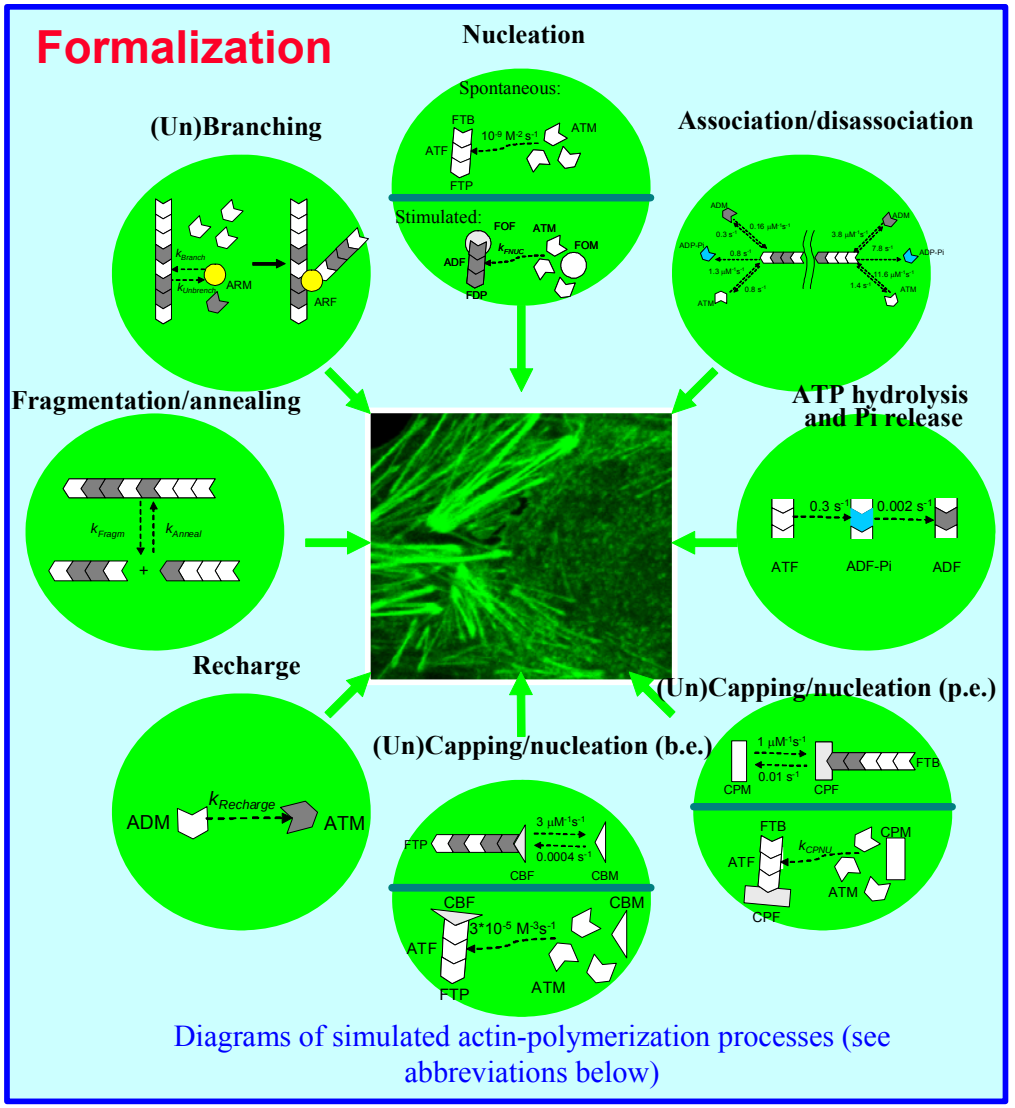

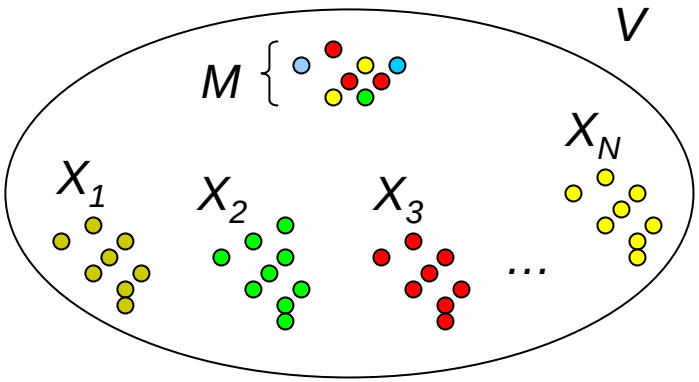

We want to solve the following problem:
To find the time evaluation of N chemical species $X_1,\ldots, X_N$ interacting via M chemical channels in a fixed volume V.

Deterministic model

Ordinary differential equations

$$\frac{dX_1}{dt} = f_1(X_1,\ldots,X_N)$$

$$\frac{dX_2}{dt} = f_2(X_1,\ldots,X_N)$$

...

$$\frac{dX_N}{dt} = f_N(X_1,\ldots,X_N)$$

Stochastic model

Stochastic master equation

$$\frac{dP(\eta,t)}{dt} = \sum_{\xi}\Pi(\xi,\eta)P(\xi,t) - \sum_{\xi}\Pi(\eta,\xi)P(\eta,t)$$

$$\eta = \{X_1,\ldots,X_N\},$$
$$\xi = \{X'_1,\ldots,X'_N\}$$

Direct calculation

$$X_i(t) = \sum_{X_1}\ldots\sum_{X_N} X_i P(X_1,\ldots,X_N,t)$$

Monte Carlo simulation

$$P'(\tau,\mu,t)d\mu$$

Стохастическая модель

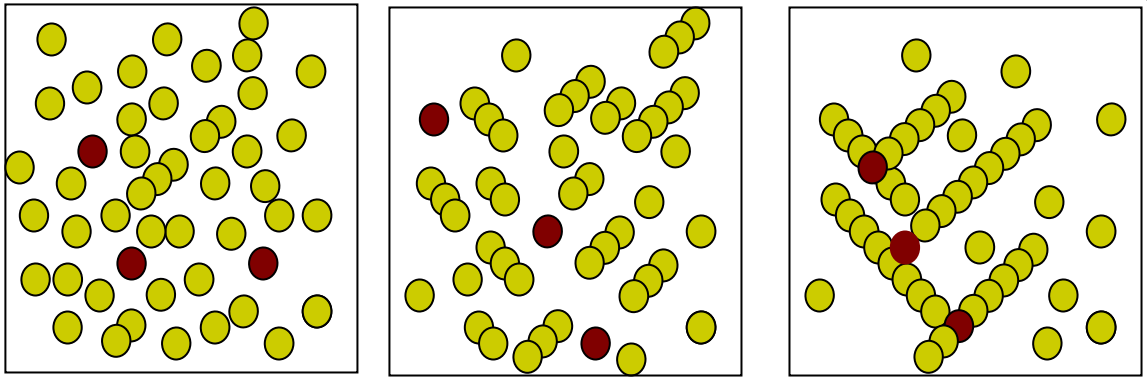

$$P'(\tau,\mu,f,p,t) = P_1(\tau)P_2(\mu\,|\,\tau)P_3(f\,|\,\tau,\mu)P_4(p\,|\,\tau,\mu,f)$$

$$P_1(\tau) = \sum_{i=1}^{M} a_i e^{\sum_{i=1}^{M} a_i \tau}$$

$$P_2(\mu\,|\,\tau) = a_\mu \Big/ \sum_{i=1}^{M} a_i$$

$$P_3(f\,|\,\tau,\mu) = \varphi_f(a_1,\ldots,a_M)$$

$$P_4(p\,|\,\tau,\mu,f) = \varphi_p(a_1,\ldots,a_M)$$

$$a_i = k_i\left(10^{-6} N_A V\right)^{1-n_i} \prod_{j=1}^{n_i} X_j$$

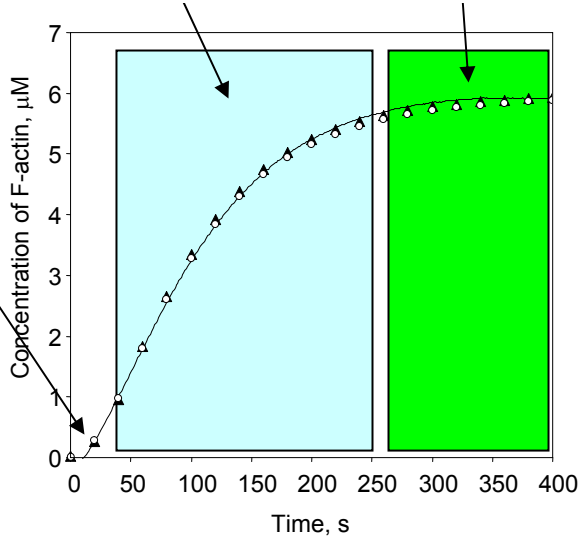

In vitro

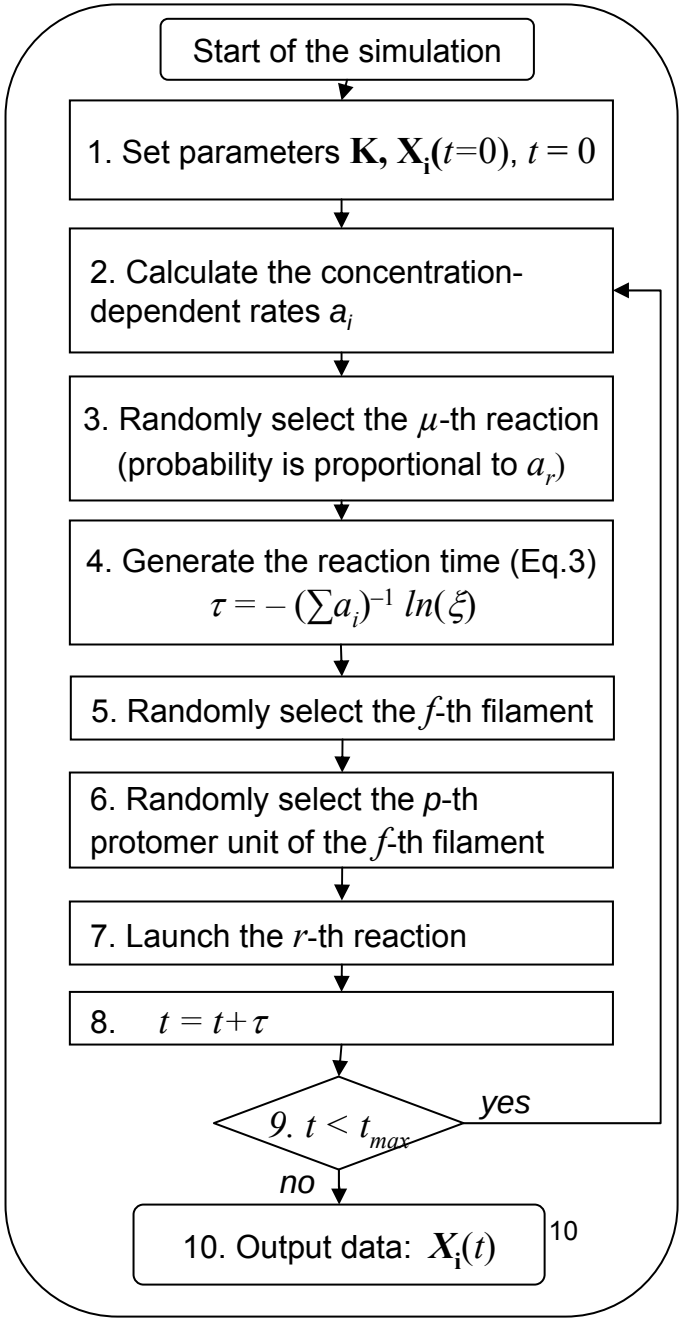

Actin fluorescence-pyrene assay in the presence of capping protein

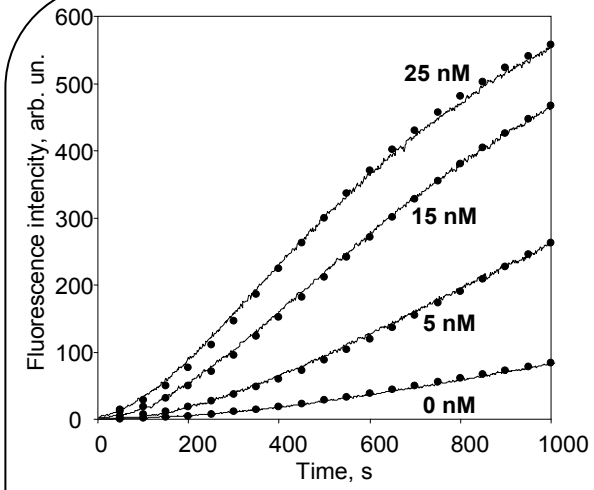

$$\begin{cases} \dfrac{d[ATF]}{dt} = 3k_{SNUC}\left(A-[ATF]-\dfrac{k_{DITB}}{k_{ASTB}}\right)^3 + 3k_{CBNU}\left(A-[ATF]-\dfrac{k_{DITB}+k_{DITP}}{k_{ASTB}+k_{ASTP}}\right)^3 (C-[CBF]) + \\ + k_{ASTB}[FTB]\cdot\left(A-[ATF]-\dfrac{k_{DITB}}{k_{ASTB}}\right) + k_{ASTP}([FTB]+[CBF])\left(A-[ATF]-\dfrac{k_{DITP}}{k_{ASTP}}\right) \\ \dfrac{d[FTB]}{dt} = k_{SNUC}\left(A-[ATF]-\dfrac{k_{DITB}}{k_{ASTB}}\right)^3 - k_{ASCB}[FTB](C-[CBF]) + k_{DICB}[CBF] \\ \dfrac{d[CBF]}{dt} = k_{CBNU}\left(A-[ATF]-\dfrac{k_{DITB}+k_{DITP}}{k_{ASTB}+k_{ASTP}}\right)^3 (C-[CBF]) + k_{ASCB}[FTB](C-[CBF]) - k_{DICB}[CBF] \end{cases}$$

Lines (−) are the experimental data.
Symbols (●▲) are simulation results.

Carlsson, A. E. et al. 2004. Biophys J 86:1074-1081.

ActinSimChem

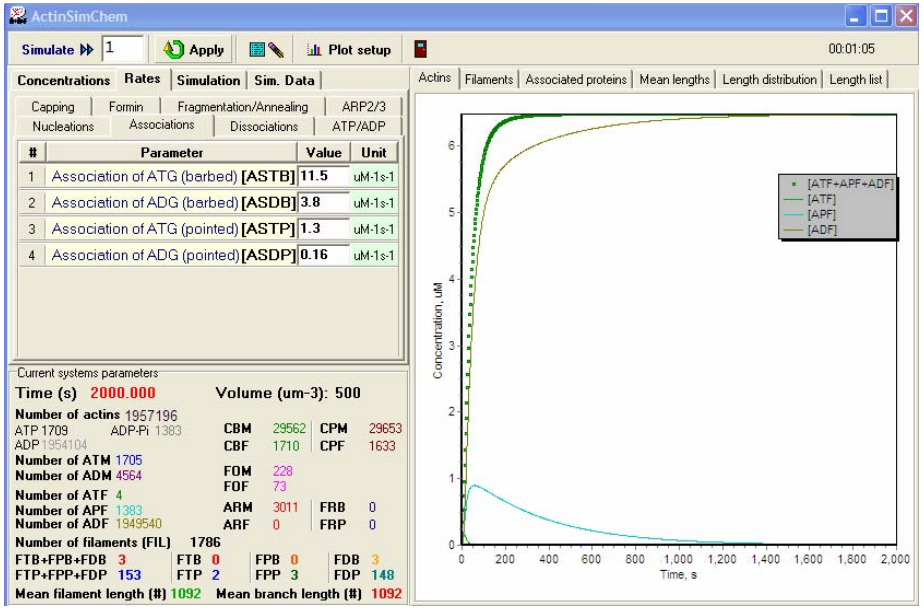

Biophys Chem 2009, vol 140, p. 24

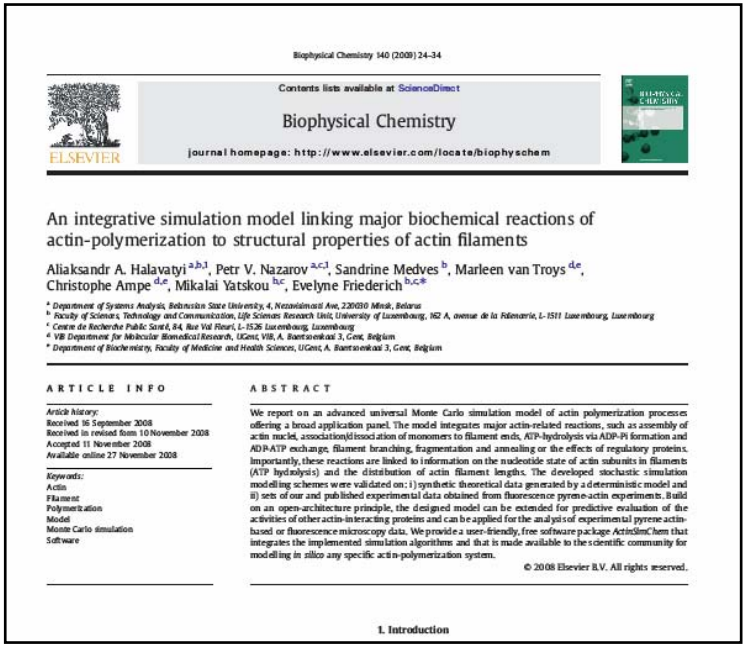

Biophysical Chemistry 140 (2009) 24–34

Contents lists available at ScienceDirect

Biophysical Chemistry

journal homepage: http://www.elsevier.com/locate/biophyschem

An integrative simulation model linking major biochemical reactions of actin-polymerization to structural properties of actin filaments

Aliaksandr A. Halavatyi [a,b,1], Petr V. Nazarov [a,c,1], Sandrine Medves [b], Marleen van Troys [d,e], Christophe Ampe [d,e], Mikalai Yatskou [b,c], Evelyne Friederich [b,c,*]

[a] Department of Systems Analysis, Belarusian State University, 4, Nezavisimosti Ave, 220030 Minsk, Belarus
[b] Faculty of Sciences, Technology and Communication, Life Sciences Research Unit, University of Luxembourg, 162 A, avenue de la Faïencerie, L-1511 Luxembourg, Luxembourg
[c] Centre de Recherche Public Santé, 84, Rue Val Fleuri, L-1526 Luxembourg, Luxembourg
[d] VIB Department for Molecular Biomedical Research, UGent, VIB, A. Baertsoenkaai 3, Gent, Belgium
[e] Department of Biochemistry, Faculty of Medicine and Health Sciences, UGent, A. Baertsoenkaai 3, Gent, Belgium

ARTICLE INFO

Article history:
Received 16 September 2008
Received in revised form 10 November 2008
Accepted 11 November 2008
Available online 27 November 2008

Keywords:
Actin
Filament
Polymerization
Model
Monte Carlo simulation
Software

ABSTRACT

We report on an advanced universal Monte Carlo simulation model of actin polymerization processes offering a broad application panel. The model integrates major actin-related reactions, such as assembly of actin nuclei, association/dissociation of monomers to filament ends, ATP-hydrolysis via ADP-Pi formation and ADP-ATP exchange, filament branching, fragmentation and annealing or the effects of regulatory proteins. Importantly, these reactions are linked to information on the nucleotide state of actin subunits in filaments (ATP hydrolysis) and the distribution of actin filament lengths. The developed stochastic simulation modelling schemes were validated on: i) synthetic theoretical data generated by a deterministic model and ii) sets of our and published experimental data obtained from fluorescence pyrene-actin experiments. Build on an open-architecture principle, the designed model can be extended for predictive evaluation of the activities of other actin-interacting proteins and can be applied for the analysis of experimental pyrene actin-based or fluorescence microscopy data. We provide a user-friendly, free software package *ActinSimChem* that integrates the implemented simulation algorithms and that is made available to the scientific community for modelling *in silico* any specific actin-polymerization system.

1. Introduction

Люминесцентная микроскопия

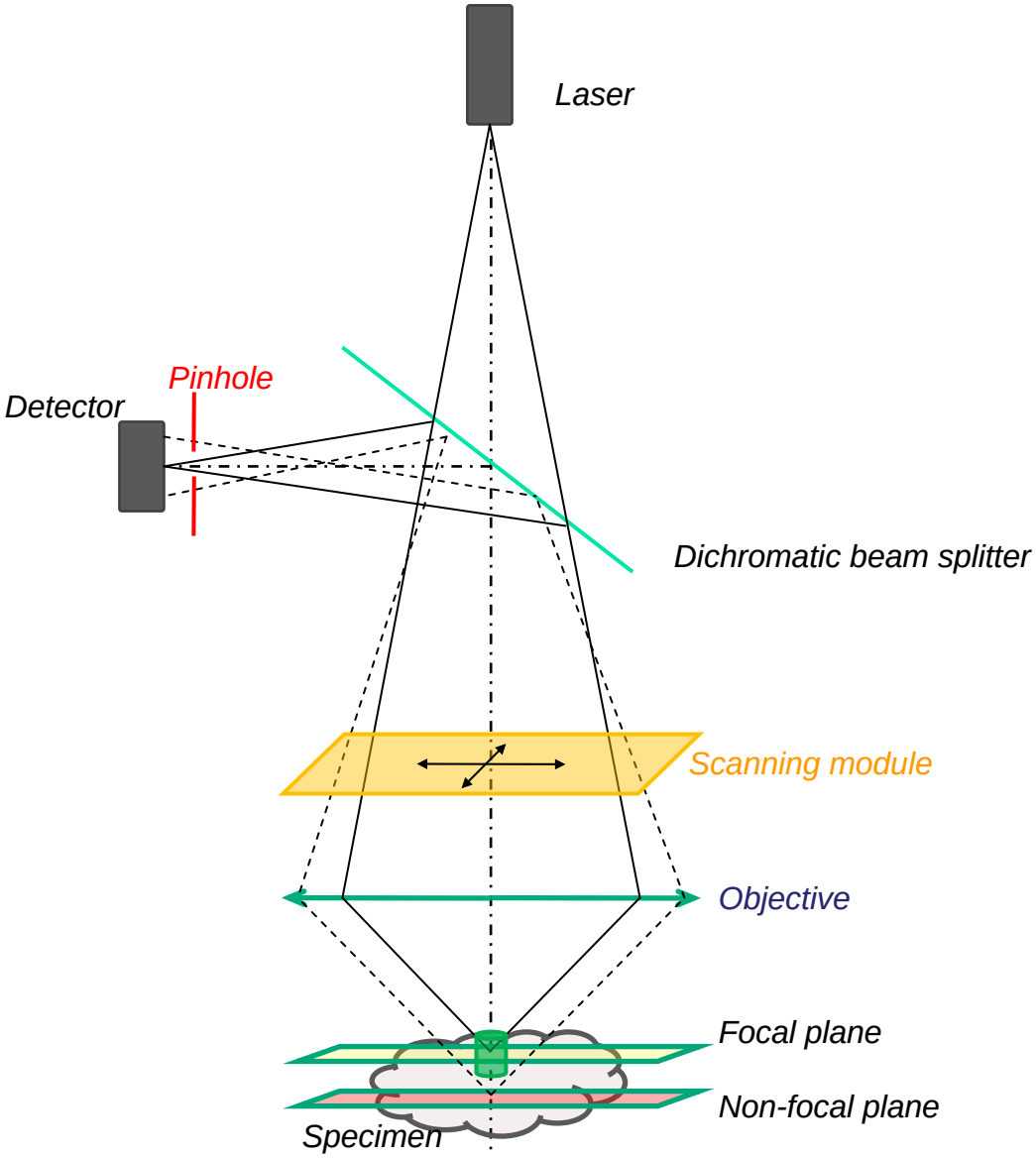

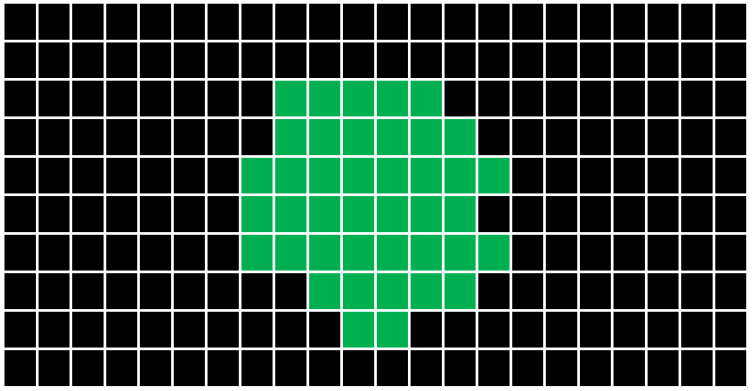

- Parameters
  - Laser power
  - Pixel dwell time
  - Image size
  - Pixel size (resolution)
  - Pinhole size
  - Detector sensitivity

Люминесцентная микроскопия

Actin-GFP

Actin-GFP + an added protein

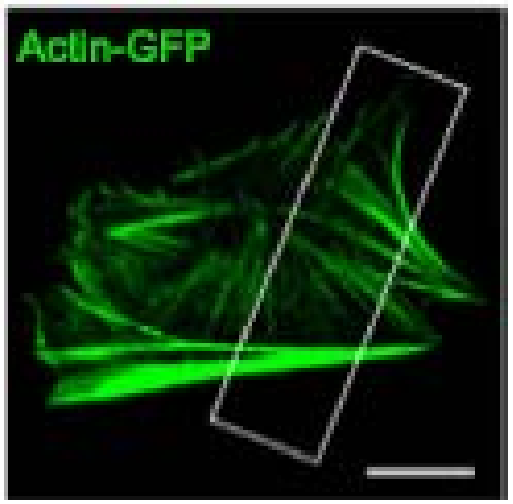

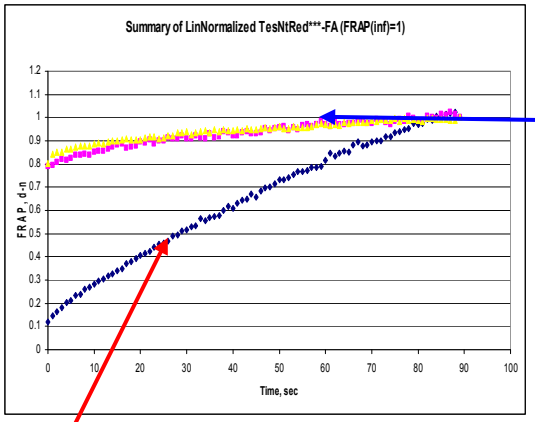

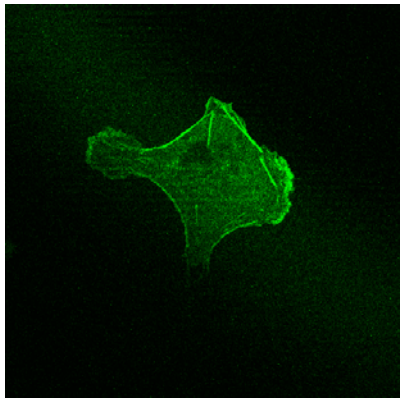

PLoS One 2010, vol 5 issue 2

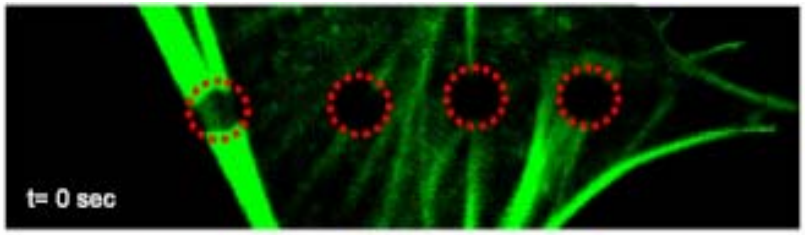

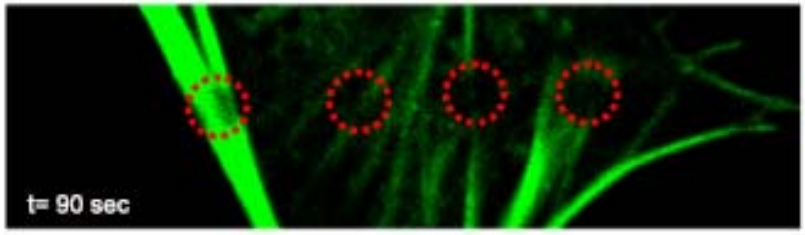

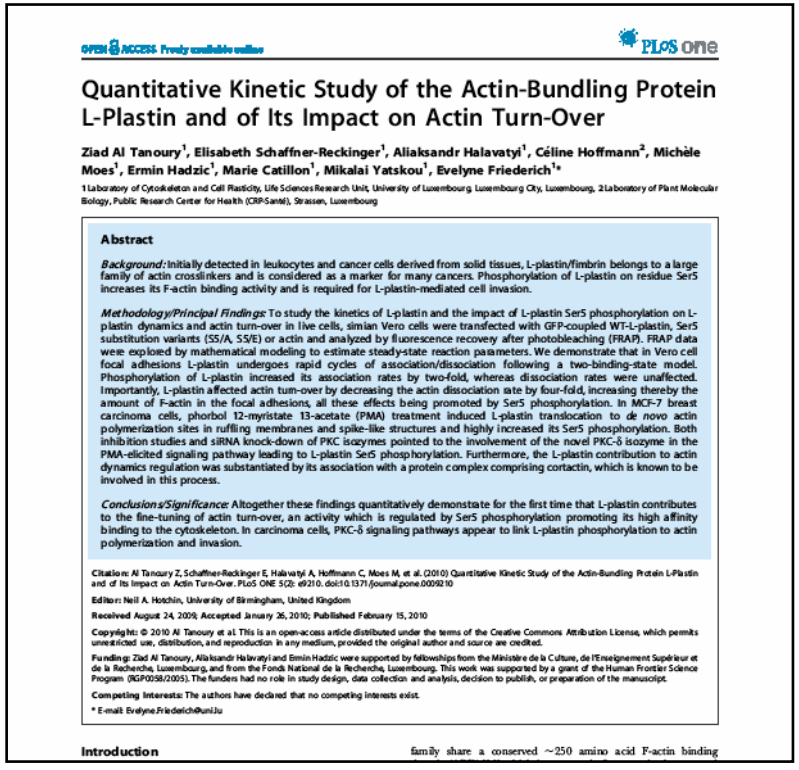

OPEN ACCESS Freely available online

PLoS one

Quantitative Kinetic Study of the Actin-Bundling Protein L-Plastin and of Its Impact on Actin Turn-Over

Ziad Al Tanoury[1], Elisabeth Schaffner-Reckinger[1], Aliaksandr Halavatyi[1], Céline Hoffmann[2], Michèle Moes[1], Ermin Hadzic[1], Marie Catillon[1], Mikalai Yatskou[1], Evelyne Friederich[1]*

1 Laboratory of Cytoskeleton and Cell Plasticity, Life Sciences Research Unit, University of Luxembourg, Luxembourg City, Luxembourg, 2 Laboratory of Plant Molecular Biology, Public Research Center for Health (CRP-Santé), Strassen, Luxembourg

Abstract

Background: Initially detected in leukocytes and cancer cells derived from solid tissues, L-plastin/fimbrin belongs to a large family of actin crosslinkers and is considered as a marker for many cancers. Phosphorylation of L-plastin on residue Ser5 increases its F-actin binding activity and is required for L-plastin-mediated cell invasion.

Methodology/Principal Findings: To study the kinetics of L-plastin and the impact of L-plastin Ser5 phosphorylation on L-plastin dynamics and actin turn-over in live cells, simian Vero cells were transfected with GFP-coupled WT-L-plastin, Ser5 substitution variants (S5/A, S5/E) or actin and analyzed by fluorescence recovery after photobleaching (FRAP). FRAP data were exploed by mathematical modeling to estimate steady-state reaction parameters. We demonstrate that in Vero cell focal adhesions L-plastin undergoes rapid cycles of association/dissociation following a two-binding-state model. Phosphorylation of L-plastin increased its association rates by two-fold, whereas dissociation rates were unaffected. Importantly, L-plastin affected actin turn-over by decreasing the actin dissociation rate by four-fold, increasing thereby the amount of F-actin in the focal adhesions, all these effects being promoted by Ser5 phosphorylation. In MCF-7 breast carcinoma cells, phorbol 12-myristate 13-acetate (PMA) treatment induced L-plastin translocation to *de novo* actin polymerization sites in ruffling membranes and spike-like structures and highly increased its Ser5 phosphorylation. Both inhibition studies and siRNA knock-down of PKC isozymes pointed to the involvement of the novel PKC-δ isozyme in the PMA-elicited signaling pathway leading to L-plastin Ser5 phosphorylation. Furthermore, the L-plastin contribution to actin dynamics regulation was substantiated by its association with a protein complex comprising cortactin, which is known to be involved in this process.

Conclusions/Significance: Altogether these findings quantitatively demonstrate for the first time that L-plastin contributes to the fine-tuning of actin turn-over, an activity which is regulated by Ser5 phosphorylation promoting its high affinity binding to the cytoskeleton. In carcinoma cells, PKC-δ signaling pathways appear to link L-plastin phosphorylation to actin polymerization and invasion.

Citation: Al Tanoury Z, Schaffner-Reckinger E, Halavatyi A, Hoffmann C, Moes M, et al. (2010) Quantitative Kinetic Study of the Actin-Bundling Protein L-Plastin and of Its Impact on Actin Turn-Over. PLoS ONE 5(2): e9210. doi:10.1371/journal.pone.0009210

Editor: Neil A. Hotchin, University of Birmingham, United Kingdom

Received August 24, 2009; Accepted January 26, 2010; Published February 15, 2010

Funding: Ziad Al Tanoury, Aliaksandr Halavatyi and Ermin Hadzic were supported by fellowships from the Ministère de la Culture, de l'Enseignement Supérieur et de la Recherche, Luxembourg, and from the Fonds National de la Recherche, Luxembourg. This work was supported by a grant of the Human Frontier Science Program (RGP0058/2005). The funders had no role in study design, data collection and analysis, decision to publish, or preparation of the manuscript.

Competing Interests: The authors have declared that no competing interests exist.

* E-mail: Evelyne.Friederich@uni.lu

Introduction

family share a conserved ~250 amino acid F-actin binding

FRAP fitting model for actin polymerization

Hypothesis:
Dynamics of beach actins in filaments can be considered as **diffusivity***

$$\frac{\partial f}{\partial t} = \frac{\partial}{\partial t}\left(D \frac{\partial f}{\partial x} \right)$$

$$\frac{\partial f}{\partial t} = D_1 \frac{\partial^2 f}{\partial x^2} + D_2 \frac{\partial f}{\partial x}$$

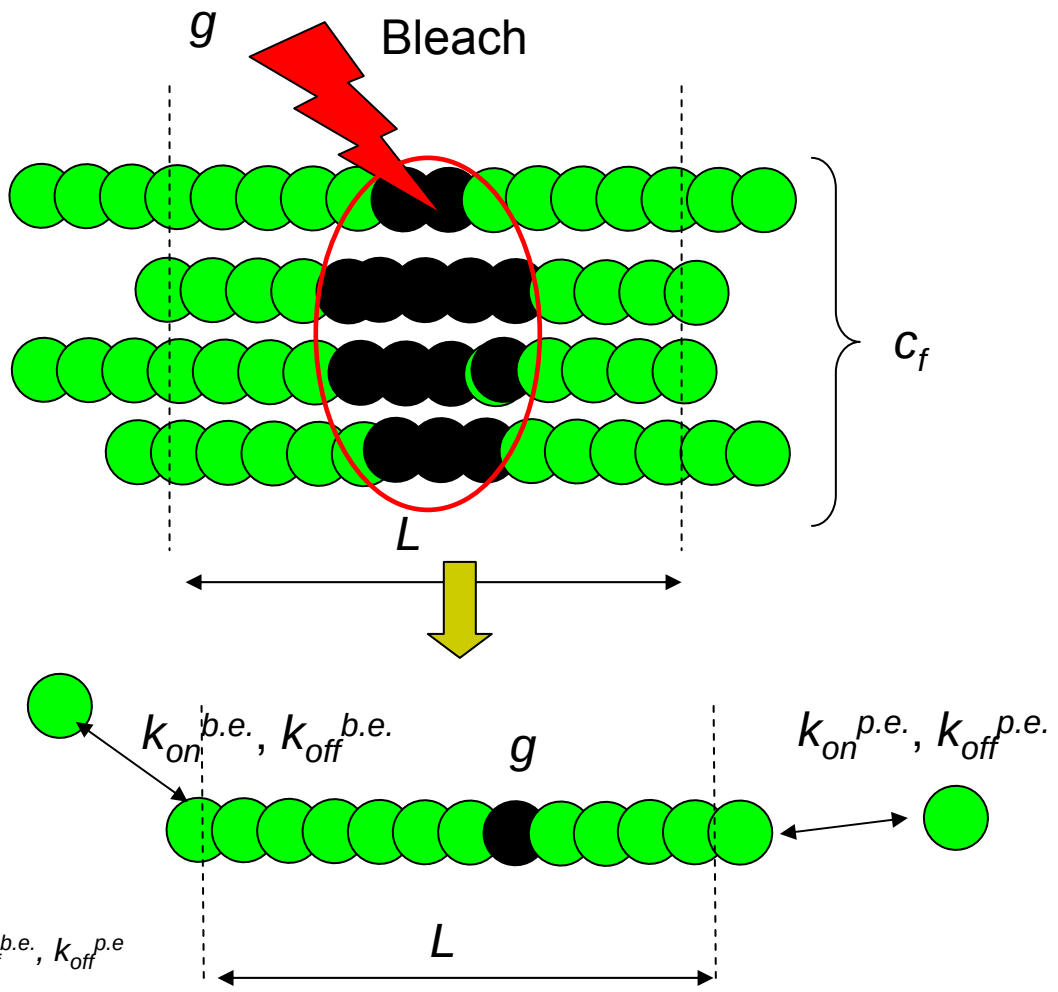

where
D_1, D_2 – are combinations of $k_{on}^{b.e.}, k_{on}^{p.e}, k_{off}^{b.e.}, k_{off}^{p.e}$
L – a mean length of filaments in the system
c_f –concentration of filamentous actins
$g(x)$ – distribution of bleaching probability along filament

Восстановление флуоресценции после обесцвечивания

$$FRAP(t) = 1 - K\int_0^L g(x)\Theta(A,x,t)dx$$

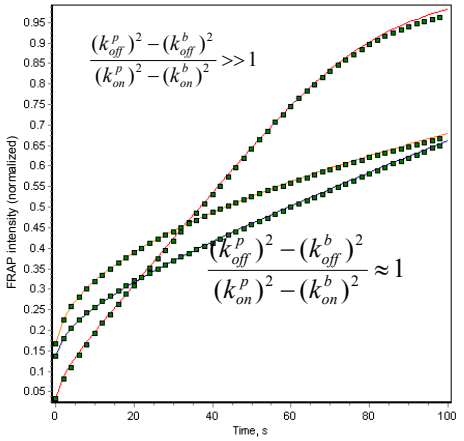

$$\Theta(A,x,t) = \Theta(L,D_1,D_2,x,t) = \Phi_{x-D_2t,\sqrt{2D_1t}}(L) - \Phi_{x_0-D_2t,\sqrt{2D_1t}}(0)$$

$$D_1 = (k_{off}^{b.e.} + k_{off}^{p.e.})/2$$

$$D_2 = [k_{off}^{b.e.} - k_{off}^{p.e.} + c_{eq}^m\left(k_{on}^{p.e.} - k_{on}^{b.e}\right)]/2$$

where

L – a mean length of filaments in the system
K – normalized concentration of filamentous actins
g(x) – distribution function of bleaching probability along filament
$c_{ss}^{\ m}$ - steady-sate concentration of free actins

Eur Biophys J 2010, vol. 39, p. 669

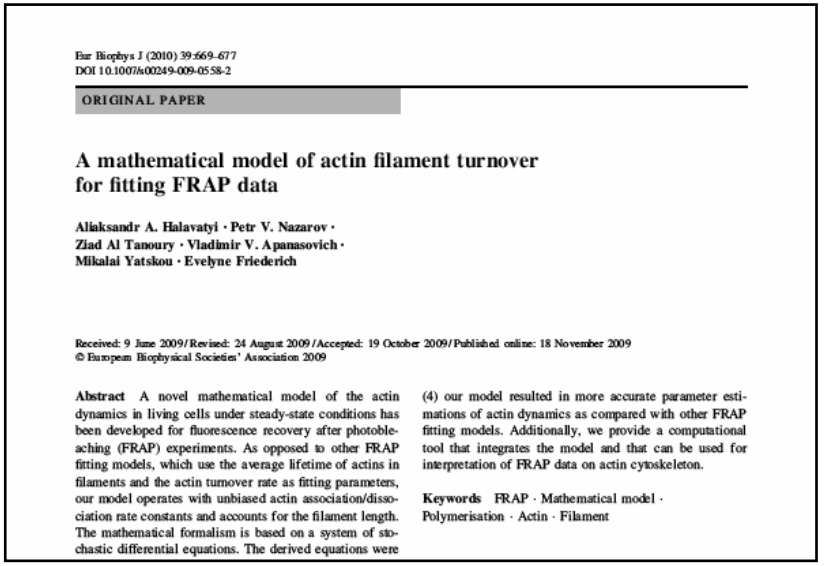

Eur Biophys J (2010) 39:669–677
DOI 10.1007/s00249-009-0558-2

ORIGINAL PAPER

A mathematical model of actin filament turnover for fitting FRAP data

Aliaksandr A. Halavatyi · Petr V. Nazarov · Ziad Al Tanoury · Vladimir V. Apanasovich · Mikalai Yatskou · Evelyne Friederich

Received: 9 June 2009 / Revised: 24 August 2009 / Accepted: 19 October 2009 / Published online: 18 November 2009

Abstract A novel mathematical model of the actin dynamics in living cells under steady-state conditions has been developed for fluorescence recovery after photobleaching (FRAP) experiments. As opposed to other FRAP fitting models, which use the average lifetime of actins in filaments and the actin turnover rate as fitting parameters, our model operates with unbiased actin association/dissociation rate constants and accounts for the filament length. The mathematical formalism is based on a system of stochastic differential equations. The derived equations were (4) our model resulted in more accurate parameter estimations of actin dynamics as compared with other FRAP fitting models. Additionally, we provide a computational tool that integrates the model and that can be used for interpretation of FRAP data on actin cytoskeleton.

Keywords FRAP · Mathematical model · Polymerisation · Actin · Filament

FRAPAnalyser

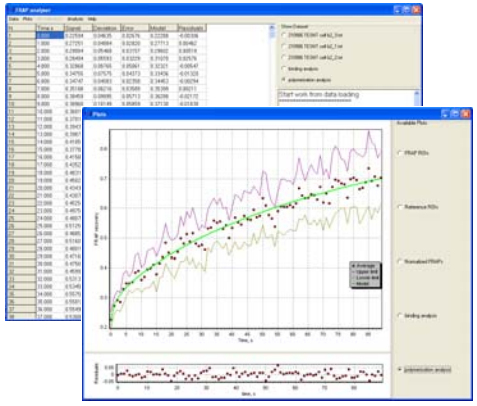

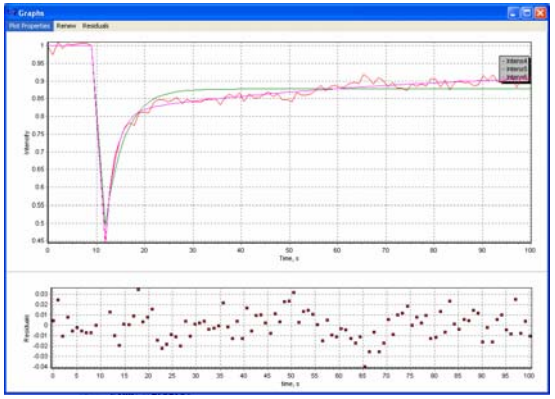

FRAPAnalyser is published in the book "Lfe Cell Imaging: A Laboratory Manual" (2010)

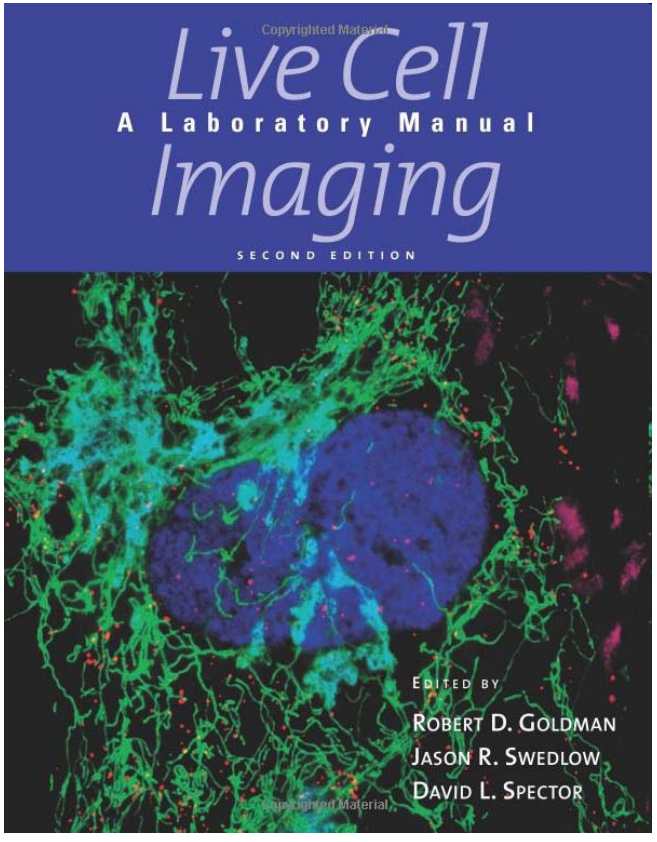

- FRAP Analyzer is the stand-alone program package that provides:
  - FRAP data input/output.
  - Multi-cells data analysis
  - Several normalization methods for the FRAP curves.
  - Data averaging and graphical visualization.
  - ***Modelling*** - diffusion models, multi-binding states models, mixed models, actin-polymerization model.
  - ***Fitting*** – by diffusion models, multi-binding states models, mixed models, actin-polymerization model.
  - Fit quality estimation of fit.

Благодарность

Проф. Кристоф Ампе, Университет Гента, Бельгия
Проф. Мэрлин Ван Трой , Университет Гента, Бельгия

Проф. Райнер Пепперкок, EMBL, Хайдельберг, ФРГ
Др. Ш. Терьюнг, Хайдельберг, ФРГ

Проф. Оливер Пох , Университет Страсбурга, Франция
Проф. Эмануэль Барийо, Институт Кюри, Париж, Франция
Др. Джон Мюллер, IGBMC, Страсбург, Франция
Др. Новиков Е., Карл-Цейс, ФРГ

Ст. преп. В.М. Лутковский, БГУ
Маг. Е. Лисица, БГУ